

*Ahmet Çağrı Bilir*  
*Ali Doğrul*  
*Nurten Vardar*



<http://dx.doi.org/10.21278/brod73408>

ISSN 0007-215X  
eISSN 1845-5859

## **AN EXTENSIVE INVESTIGATION OF FLOW CONDITIONERS INSIDE A FI-FI MONITOR**

UDC 681.533.38:621.184.22  
Original scientific paper

### **Summary**

As it is known, to provide fire protection for any type of surface vessel, external fire-fighting (EFF) systems have been commonly used for decades as well as in coastal regions. These types of systems exist on several types of vessels such as fire-fighting ships, tugboats, supply vessels and naval vessels. Flow conditioners can be used in the EFF systems to provide better performance by regulating the flow inside the fi-fi monitor. In the present study, a fire-fighting (fi-fi) monitor was designed and different flow conditioners were implemented into the fi-fi monitor. A unique flow conditioner was designed in addition to the recommended ones by ISO 5167-3 in order to improve the performance of the flow conditioner in terms of head ratio and flow rate. A commercial computational fluid dynamics (CFD) solver was used to investigate the performance of the different flow conditioners. Before comparing the numerical results of different flow conditioners, the numerical model was validated with the experimental data and verified with appropriate methods. The results showed that the unique flow conditioner successfully regulates the streamlines and it has better performance than the recommended ones by ISO 5167-3 in terms of flow rate and head ratio. As the last part of the study, the effect of unique flow conditioner length was investigated and the best length was determined.

*Key words:* *fi-fi monitor; flow conditioner; head ratio; Tube Bundle; Zanker*

### **1. Introduction**

External fire-fighting systems (EFF) are used in tug boats, naval ships, supply vessels and especially fire-fighting vessels to handle the fire protection of ships, offshore platforms, ports and coastal regions. The EFF systems consist of a power supply (main engine/diesel generator), pipes, valves, pumps and a fi-fi monitor. The system is powered by the main engine or diesel generator and the water is directed to the fi-fi monitor using various valves and pumps. Since the throw distance of the monitor is important, maritime classification societies, which are IACS members, categorize the EFF systems due to the longitudinal and horizontal throw

distance of the water at a constant flow rate. Table 1 shows the categorization rules of Bureau Veritas (BV) [1].

**Table 1** Bureau Veritas EFF system categorization rules

Parameter	FIFI I	FIFI II	FIFI III
Monitors	2	3	4
Capacity per Fi-Fi Monitor (m <sup>3</sup> /h)	1200	2400	2400
Pumps Quantity	1	2	2
Total Pump Cap. (m <sup>3</sup> /h)	2400	7200	9600
Height of Throw (m)	45	70	70
Length of Throw (m)	120	150	150

Ships have responded to many coastal and offshore fires around the world with the EFF system for years. Figure 1 shows the fire-fighting ships that intervened in the fire that occurred on the BP petroleum platform in the Gulf of Mexico in 2010. The fire is also called “The Deepwater Horizon oil spill” and is regarded as one of the largest environmental disasters and offshore fires in history. Figure 1 also shows the fire that broke out at Istanbul Haydarpaşa Train Station in Istanbul in 2010, fire-fighting ships responded with their EFF systems.



**Fig. 1** Responses of fire-fighting ships to the fire on an offshore platform and a coastal region [2], [3].

In addition to the throw distance, the flow quality is significant in the EFF systems. Pulverization of the water outside the monitor is not wanted, so the water exiting the fi-fi monitor should be homogenized inside the fi-fi monitor. Several geometric components are used in EFF system design. However, each of these components (reducer, diffuser, elbow, bend, tee junction, fitting) causes pressure loss and turbulence in the flow. The turbulence causes swirl, separation and vorticity. These instabilities in the flow cause larger pump capacity and energy consumption. For these reasons, the flow inside the fi-fi monitor should be regulated.

The flow conditioners are mainly used in pipe flows to regulate the flow and cope with measurement errors. International Organization for Standardization (ISO) [4] recommends a standard of several flow conditioner designs (Gallagher, Tube Bundle, Zanker) to provide better measurement of flow characteristics. Design definitions, test conditions and tolerance values are shown on the standard.

The experimental study of flow regulation is providing first-hand data, however, the related cost with experiment setup is generally very high. Despite this, there are several experimental studies about the flow conditioners in the open literature and some of them are summarized below briefly. To explore the effect of a complex flow profile on the performance of a multipath ultrasonic flow meter, Brown and Griffith [5] examined experimentally separate

flow conditioner designs and proposed a new design intended for use with ultrasonic flowmeters. According to their measurements, the results with the new conditioner were found equal to the Laws-type plate, but, they accomplished it with less than half the pressure loss. Using flow conditioners not only improves flowmeter performance but also reduces the piping cost. Xiong et al. [6] carried out a study to compare different types of flow conditioners and lengths experimentally. They highlighted that the perforated plates are more efficient than the tube bundle. Another similar comparing experimental study was conducted by Laribi et al. [7]. According to this study, each flow conditioner affects a specific flow parameter. The most appropriate results were obtained by the Laws perforated plate for the velocity profile. For the swirl angle, the best results were acquired by the tube bundle, whereas the Etoile is more suitable on the turbulence intensity profile. It is concluded that a combination of different flow conditioners can affect the flow parameters. Laws and Quazzane [8] made a detailed experimental investigation with different flow conditioner types and lengths to observe flow conditioner performance in terms of flow quality such as the velocity, streamlines and turbulence intensity. They expressed that the lengths affect the flow conditioner efficiency. Moreover, they had better flow quality with Law's and honeycomb combined plates than Zanker's. Razali et al. [9] carried out their experimental study to investigate the porosity of the flow conditioner effect in pipe flow. They showed that the more porosity caused the less pressure drop. Moreover, pressure drop increased when the flow rate and velocity increased.

On the other hand, computational fluid dynamics (CFD) methods are getting more and more attention in the modeling of turbulent flow in pipes not only with the recent development in computational capability but also its simplicity and cost-effectiveness. Chen and Liu [10] investigated the performance of an Etoile flow conditioner downstream of a vortex generator, finding that the Etoile conditioner helps to modify the abnormal flow field. The authors designed a new flow conditioner and obtained better performance with the new design when compared with the Etoile conditioner in a specific range of Reynolds numbers. Lahadi et al. [11] presented a study based on the effects of fractal grid-generated turbulence on turbulent intensity and pressure drop in pipe flow. Three plates with different porosities were compared. It was found that the low porosity plate can handle higher turbulence intensity. Pramiyanti et al. [12] also carried out a numerical study with three different flow conditioner lengths. The results showed that the perforated plate can be used to eliminate the swirl and generate a standard velocity profile for internal flows. Zaryankin et al. [13] investigated the widely used current flow conditioners in pressurized water flow in pipes numerically. Then they proposed specified flow conditioner geometries to reduce the dynamic load caused by the pressurized flow. The efficiency of the new configurations was assessed by employing the CFD methods and compared against the existing models. The results showed that the new configurations demonstrated a comparable degree of reduction of the dynamic loads thanks to better flow regulating performance with the new flow conditioner design.

To guarantee the results, some researchers made their studies include both experimental and numerical methods. Askari et al. [14] carried out a numerical and experimental study with well-known flow conditioners such as NEL, Spearman and Mitsubishi. The authors finally designed a new flow conditioner and obtained the optimum efficiency. Another study was conducted by Bayazit et al. [15]. They investigated the porosity and length effects of the flow conditioner that caused a pressure drop and flow laminarization for different Reynolds numbers in the square duct. The analyses were carried out numerically and compared with the experiment results. As a result, the flow conditioner with the optimum performance was also produced. One more numerical and experimental study comparing flow conditioner performance was done by Carpinoglu and Ozahi [16]. They implemented Etoile, Perforated Plate and Tube Bundle flow conditioners on an air compressor system and investigated the

pressure losses and turbulence intensity in different Reynolds numbers. While the tube bundle had the minimum pressure losses, the perforated plate had the maximum pressure losses for all tested Reynolds Number conditions. Liu et al [17] conducted their numerical and experimental studies by changing the orifice angle of the ISO-type flow conditioner to eliminate the turbulent effect caused by the ball valve in pipe flow. They obtained that the rectified flow conditioner had better performance than standard ISO-type plates. Chen et al. [18] investigated the flow distortion effect on the measurement accuracy of the ultrasonic gas flowmeter experimentally and numerically, and the physical mechanism of characteristic parameters on measurement accuracy was explored. Dramatically they showed that the flow conditioners positive effect on the complex flow by comparing the flow without the conditioner.

Within this, there are few studies found in the literature focusing on the flow conditioners in fi-fi monitors and their industrial applications. Hou et al. [19] conducted the flow through a fi-fi monitor nozzle numerically. The researchers optimized the conical nozzle angle in terms of pressure and velocity distributions. A similar study was made by Hu et al. [20]. They investigated the jet flow characteristics of a fi-fi monitor, numerically. Different cross-sectional areas, fi-fi monitor diameters and inlet pressure values were compared to observe the effects on the jet flow. After the design optimization, they produced a fi-fi monitor for the experimental study and compared the numerical results. Choudhury and Rodriguez [21] made research focusing on the optimization of the pathway design of the fi-fi monitor based on the numerical method. The authors compared the pressure loss of different designs.

To the best of the authors' knowledge, there is a lack of study about fi-fi monitors and their flow characteristics. Within this motivation, a fi-fi monitor was designed and tested experimentally under different inlet pressures. To regulate the flow, a unique flow conditioner was designed and implemented inside the fi-fi monitor. The experiments were repeated for one flow conditioner length following the categorization rules of BV. The experimental setup was simulated numerically for verification and validation purposes. Following this, the numerical analyses were extended for a range of flow conditioner lengths for the unique flow conditioner. Zanker and tube bundle-type flow conditioners were also analyzed numerically under the same conditions and the results were compared in detail. The unique flow conditioner was found the most appropriate one in terms of mass flow rate and head ratio.

## 2. Design Methodology

All marine industrial machinery designs should be optimized meticulously in terms of dimension and weight to provide stabilization, easy operation and lower power demand. In this study, flow in the fi-fi monitor was investigated both experimentally and numerically following BV rules. Therefore, the fi-fi monitor design was highlighted in this paper. The fi-fi monitor consists of three main parts: body, pipeline, nozzle and the water in the fi-fi monitor passes through these parts respectively. Figure 2a shows the main flow volume components of the fi-fi monitor while Figure 2b shows the main dimensions of the newly designed fi-fi monitor. It should be noted that the nozzle angle is  $20^\circ$ .

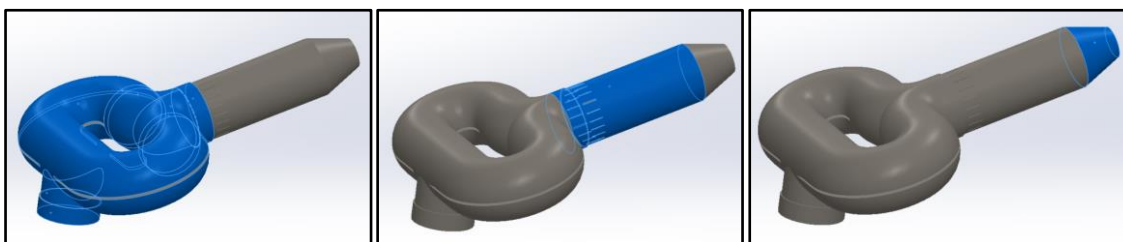


**Fig. 2a** Fi-fi monitor flow volume parts; separated body, pipeline with flow conditioner and nozzle

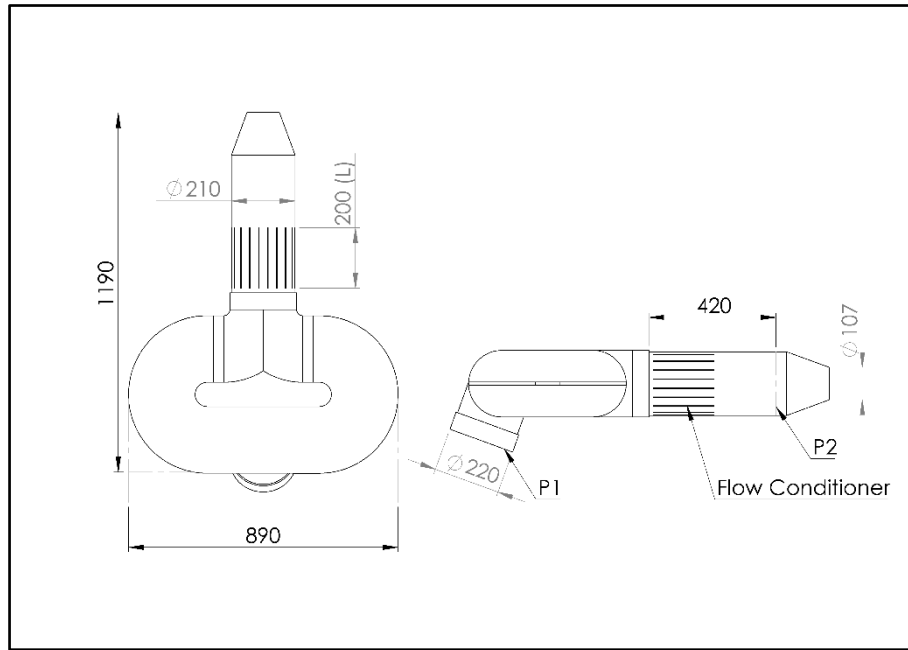


**Fig. 2b** Fi-fi monitor flow volume dimensional drawing

The body is the first part of the fi-fi monitor which water enters first. The separated body is divided into two pipelines merging again at the end of the body.

The pipeline is located between the nozzle and the body. A straight pipe is needed for laminarization on the fi-fi monitors to transmit water to the nozzle properly as a regulated flow to provide the requested water throw length. However, especially on fi-fi monitors having separated bodies, the pipeline alone is not enough for laminarization. Even the longer pipeline provides better laminarization and water throw performance, the fi-fi monitor limits the pipeline length. So, to overcome complex flow in the fi-fi monitor, a flow conditioner is placed in the pipeline. In the present study, different types of flow conditioners are modeled and simulated for different inlet pressures and flow conditioner lengths. Although pipeline length was determined as almost  $3 \cdot D$  ( $D$  is the pipe diameter), it was not enough to provide laminarization. So a flow conditioner was designed and placed into the pipeline to regulate the complex flow.

The nozzle is the last part of the fi-fi monitor. There are many types of nozzle geometries such as Pelton, reverse Pelton, Convex type, concave type and conical nozzle with different angles. Bilir et al. [22] designed five different types of fi-fi monitor nozzle with the same outlet diameter and conducted numerical analyses. They compared the reaction force in addition to velocity and pressure. Then they proposed the conical nozzle with minimum reaction force for the same boundary conditions.

Flow conditioner designs are multi-purpose and allow for variations in flow conditioner length, the number of holes, pressure loss and velocity profile as suitable for different application requirements. Despite flow conditioners recommended by ISO, the laminarization process in more complex geometries with strong curvature and rotation needs a more specific and customized flow conditioner design. Therefore, a unique flow conditioner design with different flow conditioner lengths for the fi-fi monitor was designed. A unique flow conditioner added in the fi-fi monitor pipeline with a diameter of 210 mm is divided by plates with a wall thickness of 2 mm and has a square section of 28x28mm. To reduce the fluctuation in the flow line, instead of a very short structure, the present design was made with a length of 200 mm as close to the pipe diameter. According to the flow conditioner length equation of ISO standard for flow conditioner design (Length =  $0.15 \times$  Diameter), all conditioners' lengths were designed at 31.5mm while the fi-fi monitor pipe inlet diameter is 210mm. To see the length effect in the

fi-fi monitor flow, Zanker and Tube Bundle were also redesigned with 200mm length as compatible with the unique design. After comparing the type of flow conditioner designs, the length effect study was extended for the unique design to 50mm and 100mm. Zanker, Tube Bundle and unique flow conditioners on fi-fi monitors are shown in Figure 3.

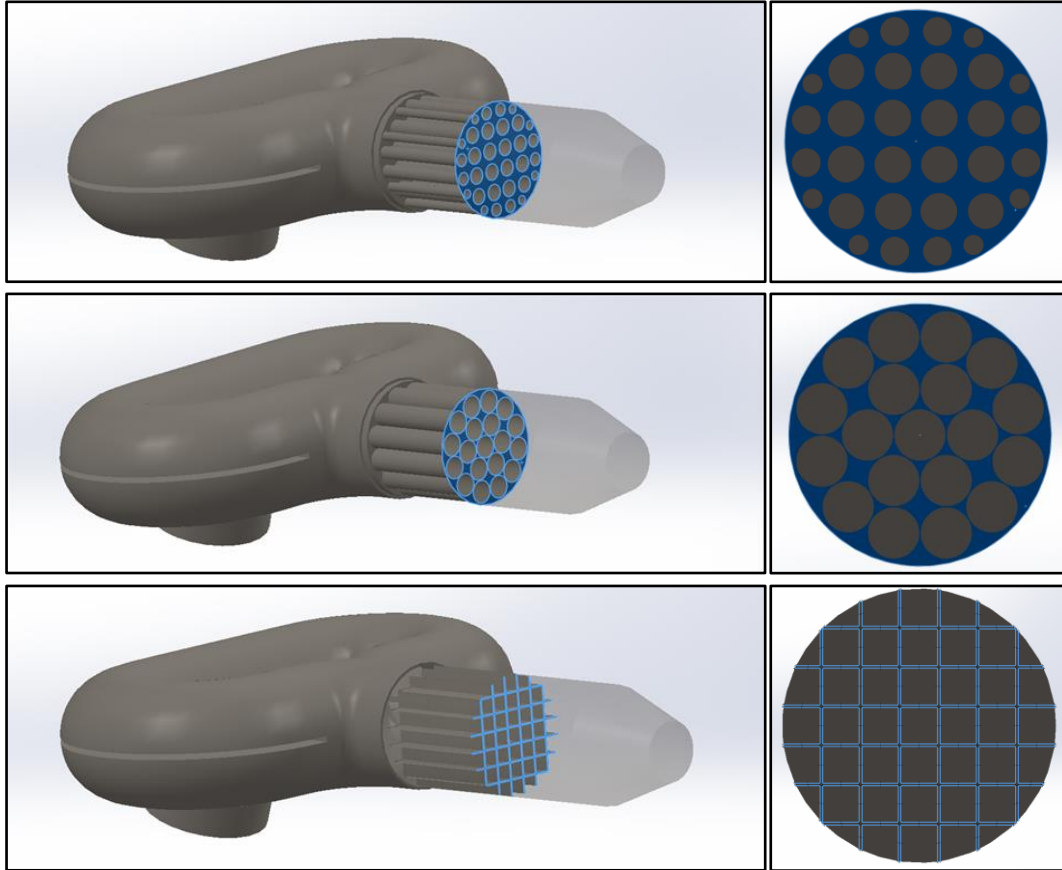


**Fig. 3** Flow conditioner designs on fi-fi monitor and cross-section view (top: Zanker, middle: Tube Bundle, bottom: Unique)

### 3. Numerical Approach

The numerical analyses were conducted using a commercial viscous flow solver, SIEMENS PLM Star CCM+. The flow was considered 3-D, incompressible and fully turbulent. Reynolds-Averaged Navier Stokes (RANS) equations were solved in an unsteady manner to mimic the temporal behavior of the flow inside the monitor system. The governing equations are the continuity and momentum equations. The continuity equation is given as:

$$\frac{\partial U_i}{\partial x_i} = 0 \quad (1)$$

The momentum equation for viscous and incompressible flow is briefly below in Cartesian coordinates and indices notation:

$$\frac{\partial U_i}{\partial t} + U_j \frac{\partial U_i}{\partial x_j} = -\frac{1}{\rho} \frac{\partial P}{\partial x_i} + \frac{\partial}{\partial x_j} \left[ \nu \left( \frac{\partial U_i}{\partial x_j} + \frac{\partial U_j}{\partial x_i} \right) \right] - \frac{\partial \overline{u_i u_j}}{\partial x_j} \quad (2)$$

Here,  $\rho$  is the fluid density,  $U_i$  is the velocity vector, m/s;  $P$  represents the pressure. The last two terms belong to the viscous stress tensor, while  $\nu$  is the kinematic viscosity.

The solution procedure was built on a semi-implicit method for pressure-linked equations (SIMPLE) type algorithm [23]. Since the flow phenomenon investigated in the present study is a separated flow, the turbulent flow was modeled using the  $k-w$  SST turbulence model. This model was employed to simulate the probable flow separations inside the fi-fi monitor. Detailed information about the model can be found in Menter [24], [25].

The numerical simulations were carried out by modeling only the fi-fi monitor since the flow is internal. The computational domain was created inside the fi-fi monitor including the body, pipe and nozzle. The entrance to the body was defined as pressure inlet (total pressure) and the exit of the nozzle was defined as pressure outlet since the experimental data was based on only pressure measurements. The remaining surfaces were set as no-slip wall. It should be noted that turbulence intensity was selected as 0.01 and turbulent viscosity ratio was selected as 10. The other properties related to the turbulence model were set as default. The boundary conditions are shown in Figure 4.

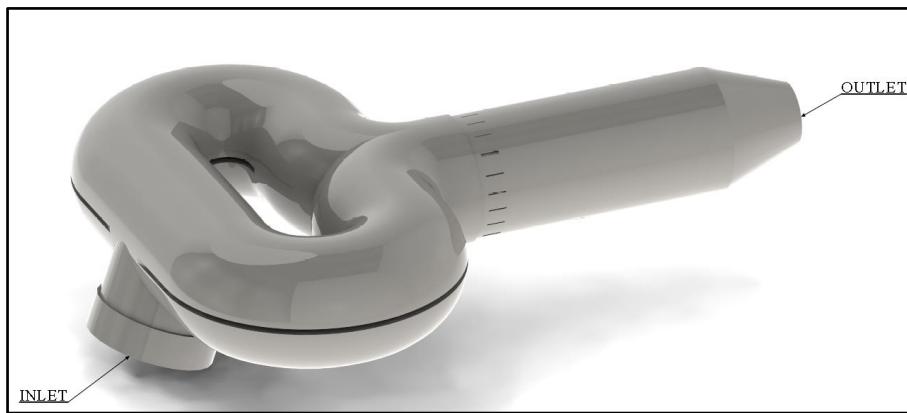


**Fig. 4** Boundary conditions

The computational domain was discretized using hexahedral elements based on the finite volume method employing the mesh wizard of the viscous flow solver. Prism layers near the wall surfaces were created and all  $y^+$  wall function was used to model the flow inside the prism layer.  $y^+$  was kept between 30 and 300 as recommended by several studies and guidelines [26], [27]. In addition to the prism layer, local mesh refinement was done around the flow conditioner inside the pipe to well-capture the flow in the upstream and downstream regions. The mesh structure sample is shown in Figure 5.

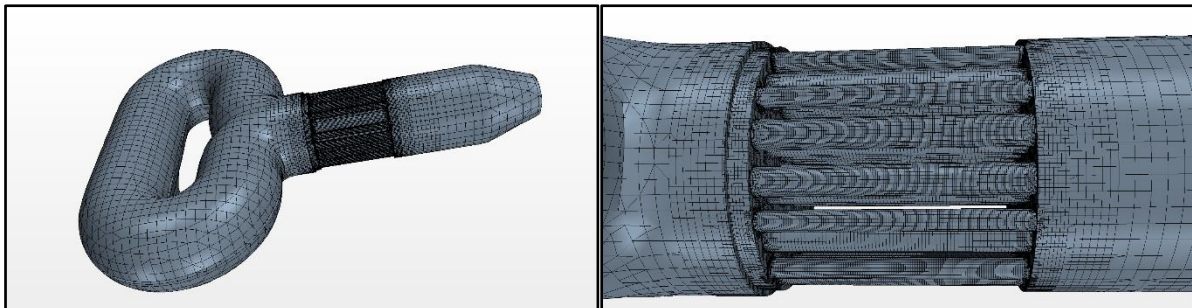


**Fig. 5** Mesh structure

#### 4. Experimental Approach

Fi-fi monitor without any flow conditioner was produced as a prototype and experimental studies were carried out. It was seen from the experiments that the flow in the fi-fi monitor

should be regulated since it was pulverized before reaching the desired throwing distance in the longitudinal direction. To defeat this problem, a 200mm unique flow conditioner was designed, implemented into the fi-fi monitor and tested experimentally. All experiments were conducted in the field of State Port Services in Tuzla, Istanbul, under the supervision of Bureau Veritas (BV) and Turkish Lloyd (TL). The experimental measurements were obtained in terms of the inlet pressure, the flow rate and the horizontal and vertical throwing distance of the water to align with the marine classification request. During the experiments, a 1 x 820 kW diesel engine, 1 x 1350 m<sup>3</sup>/h capacity centrifugal pump, a digital flow meter, pressure gauges, a gate valve and a prototype fi-fi monitor in full-scale were used. The whole measurement instruments utilized in the tests were calibrated. The experimental setup is shown in Figure 6 as a scheme and real test scene.

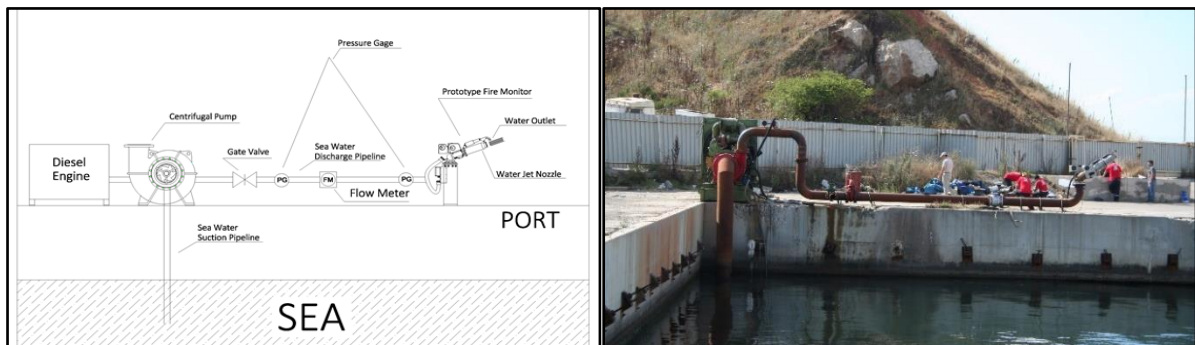


**Fig. 6** Experimental setup

The centrifugal pump transmits the seawater to the pipeline thanks to the diesel engine. The water passing through the relevant pipeline finally comes to the fi-fi monitor and is thrown into the atmosphere to reach the fire area. The experimental setup is very similar to the EFF system application on ships. Scenes during experiments are shown in Figure 7.



**Fig. 7** Scenes from the experiments

During the experiment, the fi-fi monitor was fixed in vertical and horizontal directions. Experimental studies showed that the fi-fi monitor has a better stand at an angle of 35° with the ground to throw the water to the maximum distance in the horizontal direction. In line with this information observed from the experiments, the other experimental studies were conducted in the same conditions. Experiments were carried out at different pressure values as 6bar, 7bar, 8bar, 9bar and 10bar. The pressure value was obtained at the entrance of the fi-fi monitor and the flow rate was noted. The horizontal throwing distances and flow rates obtained from the experiments are listed in Table 2.



**Table 2** Experimental results of the fi-fi monitor equipped with 200mm unique flow conditioner

Inlet pressure (bar)	Flow rate (m <sup>3</sup> /h)	Throwing distance (m)
6	930	90
7	990	100
8	1075	110
9	1130	115
10	1200	130

The experimental results of the 200mm flow conditioner satisfied the BV rules. While the inlet pressure was 10 bar, the fi-fi monitor threw the water at 1200 m<sup>3</sup>/h to a 130-meter horizontal distance. While the experiments with the fi-fi monitor having a 200mm plate satisfied the regulation, the fi-fi monitor without any flow conditioner did not provide this since the water was pulverized because of turbulent flow in the fi-fi monitor. After obtaining the experimental results following maritime classification rules, the fi-fi monitor with a 200mm unique flow conditioner was successful in getting Bureau Veritas and Turkish Lloyd Marine Type Approval Certificates.

## 5. Results

In this section, the numerical uncertainty was determined by using the GCI method for a unique design flow conditioner. After this, the numerical results obtained from the unique flow conditioner for 200mm flow conditioner length were compared with the experimental data to see the validity of the numerical method. Then, the presented flow conditioner was compared with two different flow conditioners recommended by ISO 5167-3 for two lengths, numerically. Finally, the effect of the length on the performance of the monitor was investigated numerically for the unique flow conditioner.

### 5.1 Uncertainty Assessment

The numerical method is mostly checked by conducting mesh dependency studies. However, apart from this approach, numerical uncertainty has to be determined. [28] The uncertainty assessment was conducted for the unique flow conditioner at maximum inlet pressure (10 bar) and 200mm length. The uncertainty sources were selected as grid spacing and time step similar with a recent study [29]. Therefore 3 analyze sets were created by refining the grid spacing and time step size with a constant refinement factor ( $r$ ),  $\sqrt{2}$ . The convergence factor ( $R$ ) can be calculated by using Equation 3.

$$R = \frac{\varphi_2 - \varphi_1}{\varphi_3 - \varphi_2} \quad (3)$$

Here  $\varphi_3$ ,  $\varphi_2$  and  $\varphi_1$  refers to flowrates obtained from the coarse, medium and fine time step or grid spacing analyses. If the convergence factor is calculated between 0 and 1, the grid convergence index method (GCI) which is recommended AIAA [30] and ITTC [31] can be applicable. The detail information about this method can be found in related references [32], [33]. Therefore, the temporal uncertainty was calculated using the GCI method following the methodology offered by Celik et al. [33]. However, the spatial uncertainty is calculated by using Equation 4 and Equation 5 following the methodology proposed by Roache et al. [34] since the convergence factor ( $R$ ) is calculated between 0 and -1.

$$E = \frac{f_2 - f_1}{1 - r^p} \quad (4)$$

$$U_N = |E| \cdot F_s \quad (5)$$

Here,  $f_2$  and  $f_1$  are the scalar solutions of coarse and fine grid structures, respectively.  $F_s$  is the safety factor and taken as 3.  $r$  is  $\sqrt{2}$  and apparent order ( $p$ ) is calculated by GCI methodology given in Roache et al. [35].  $U_N$  is the uncertainty value.

**Table 3.** Spatial and temporal uncertainty of unique flow conditioner

Parameter	Spatial	Temporal
$N_{fine}$	428887	0.010
$N_{medium}$	317792	0.014
$N_{coarse}$	249604	0.020
$\varphi_{fine} (m^3 / h)$	1219.7	1219.7
$\varphi_{medium} (m^3 / h)$	1232.4	1222.8
$\varphi_{coarse} (m^3 / h)$	1087.3	1228.3
$U_N$ (%)	0.466	0.410

The element numbers and time step sizes of coarse, medium and fine simulations are listed in Table 3. Table 3 also gives the uncertainty values in terms of grid spacing and time step size. Here,  $N_i$  is the total grid number and/or time step size in accordance with the discretization type. It can be clearly understood from Table 3 that the unique flow conditioner design has less than 0.5% uncertainty values in terms of both spatial and temporal manners.

## 5.2 Validation with the Experiment

As mentioned before, the experiments were conducted under the supervision of BV and TL in the field of State Port Services in Tuzla, Istanbul. To reach a general perspective and ensure the validity of the numerical results, the experiments were repeated for different inlet pressures. The configuration used in the experiments has a 200 mm length for a unique flow conditioner. Figure 8 shows the comparison of the numerical results and experimental data in terms of inlet pressures. Here, EFD depicts the experimental fluid dynamics while CFD stands for computational fluid dynamics.

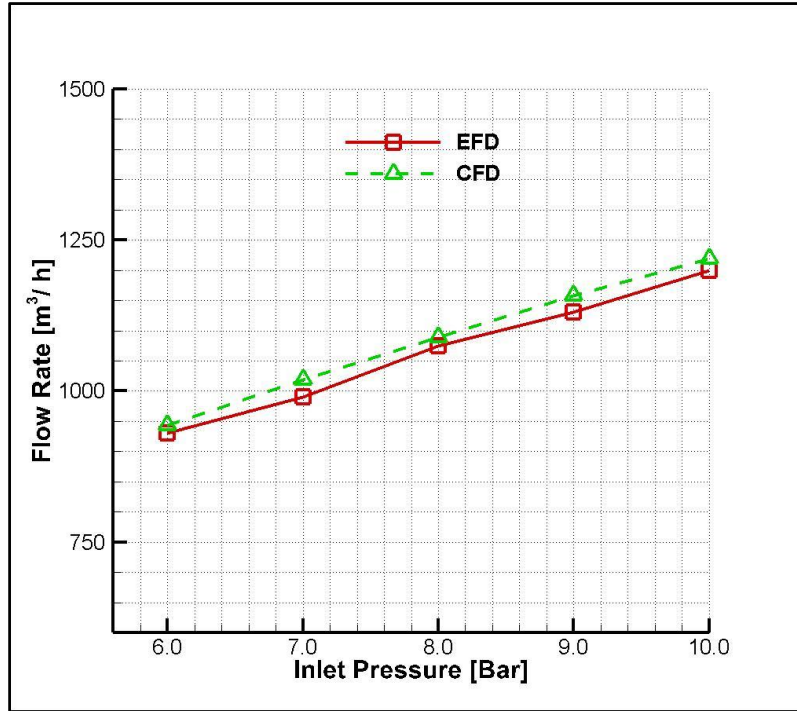


**Fig. 8** The comparison of EFD and CFD

It can be easily concluded from Figure 8 that the experimental data and the numerical results have good agreement in terms of flow rate for different inlet pressures. While the numerical method computes the flow rates higher than the experiments, the relative differences for all cases are under 3% which proves that the numerical method is capable to represent the experiment with a high order of accuracy. The numerical values of this comparison were listed in Table 4.

**Table 4** The flow rates obtained from EFD and CFD

Inlet Pressure [bar]	EFD [m <sup>3</sup> / h]	CFD [m <sup>3</sup> / h]	Relative Difference [%]
6	930	942.7	1.36
7	990	1018.7	2.89
8	1075	1089.1	1.31
9	1130	1157.5	2.43
10	1200	1219.7	1.64

### 5.3 Comparison of Different Flow Conditioners

After the validation of the numerical method with the experiments, the numerical study was repeated for different flow conditioners as mentioned before. The test matrix is listed in Table 5.

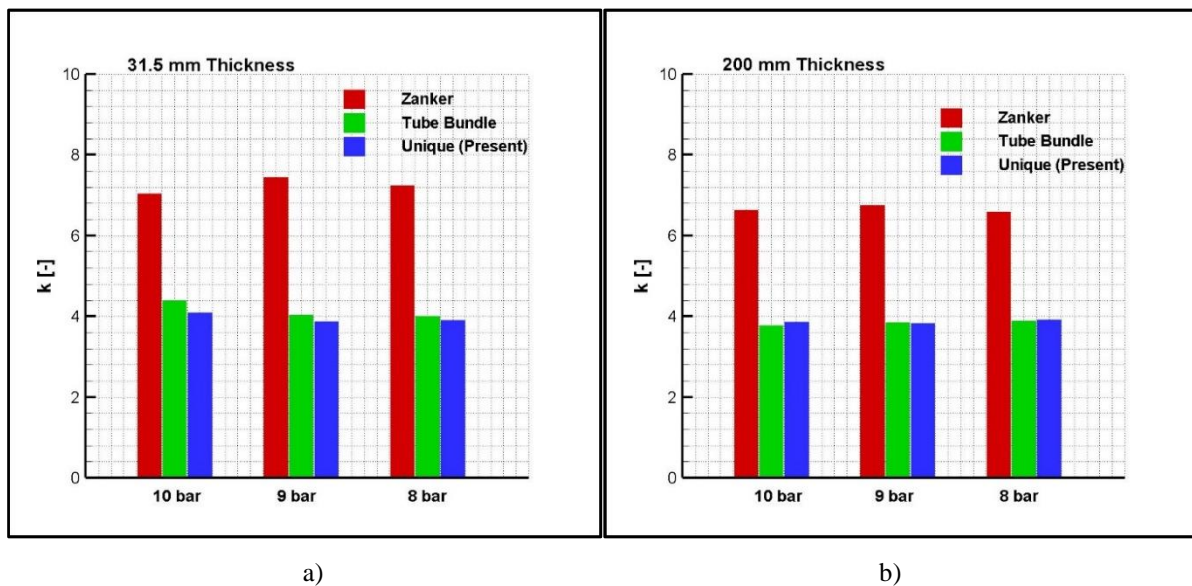
**Table 5.** The test matrix for different flow conditioners

Flow Conditioner	Length [mm]	Inlet Pressure [bar]
<i>Zanker</i>	31.5 200	8, 9, 10
<i>Tube Bundle</i>	31.5 200	8, 9, 10
<i>Unique (Present)</i>	31.5 200	8, 9, 10

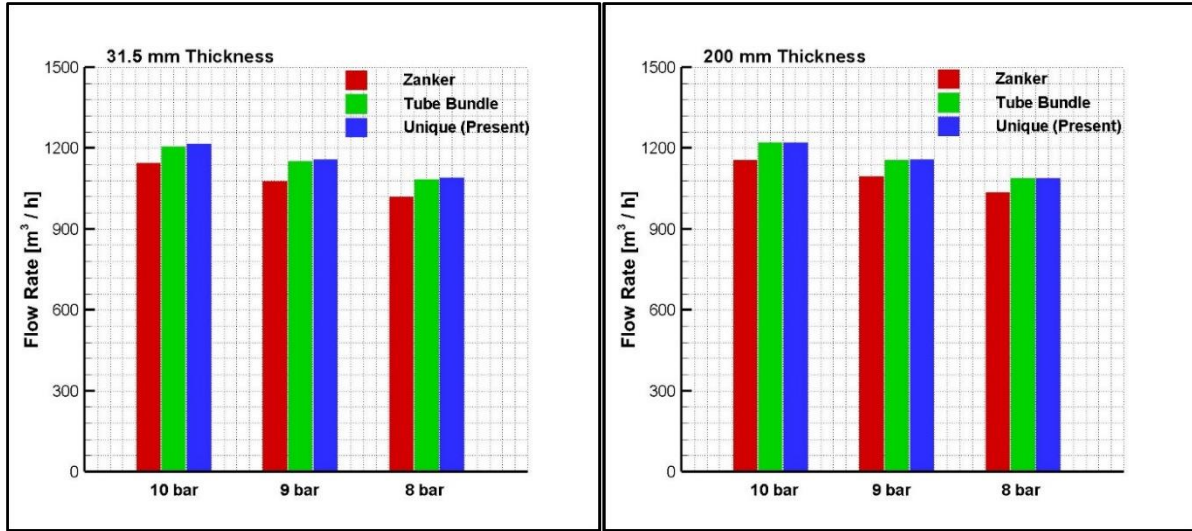
To make a fair comparison, all numerical analyses were performed for the same boundary conditions and the meshing strategy mentioned in the previous sections. The non-dimensional head ratio ( $k$ ) was calculated for each analysis to reach a general conclusion about the effect of the flow conditioner. It can be calculated by using Equation (6) where  $V$ ,  $\rho$  and  $P_1$  represent the inlet velocity (m/s), water density (kg/m<sup>3</sup>) and the inlet pressure (Pa), respectively. It should be noted that  $P_2$  depicts the average pressure measured from the beginning of the plates after 2 pipe diameters in the axial direction.

$$k = 2 \frac{P_2 - P_1}{\rho V^2} \quad (6)$$

In Figure 9, the non-dimensional head ratio is compared for different flow conditioners for different inlet pressures. The head ratio values of Zanker are the largest ones while the results of other flow conditioners are similar. Although the Tube Bundle results are slightly lower than the unique ones for 8 bar and 10 bar for 200mm length, the results of unique ones are smaller for the other cases. Thus, it can be said that the unique flow conditioner gives better results than the other two flow conditioners in terms of head ratio within the general perspective.



**Fig. 9** The comparison of different flow conditioners for different inlet pressures in terms of the head ratio  
a) 31.5mm length, b) 200mm length



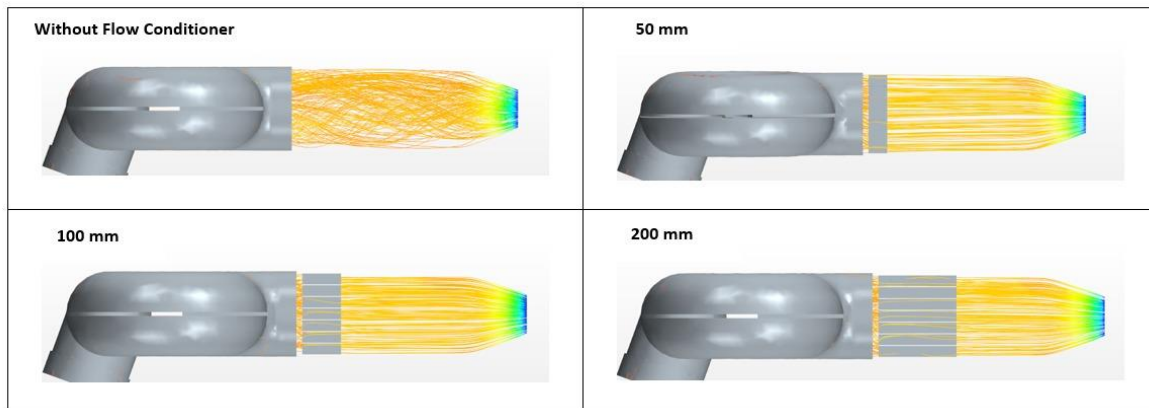
**Fig. 10** The comparison of different flow conditioners for different inlet pressures in terms of flow rate  
 a) 31.5mm length, b) 200mm length

Figure 10 shows the effect of the flow conditioner on the flow rate which is the other important performance parameter for a fi-fi monitor. The unique flow conditioner has the maximum values for all inlet pressures for smaller lengths. While the relative differences between the unique one and the Tube Bundle are very small for all inlet pressures, Zanker has minimum flow rates for all test conditions. Therefore similar conclusion to Figure 9 can be made for Figure 10. In other words, the unique flow conditioner design has better results than the other ones in general considering flow rates. According to Figures 9 and 10, the Zanker design is not appropriate for water flow regulation in EFF systems.

#### 5.4 Effect of Flow Conditioner Length on Fi-Fi Monitor Performance

Considering the conclusions made in the previous section, the unique flow conditioner design was selected to see the effect of the flow conditioner length on the monitor performance. Firstly, to deeply understand the effect of the flow conditioner on streamlines was observed.

The streamlines for different flow conditioner lengths are shown for 10 bar inlet pressure in Figure 11. According to this figure, the existence of the flow conditioner has an incredibly positive effect to regulate the flow in the fi-fi monitor regardless of the length. However, any considerable difference is not observed for the different flow conditioner lengths.



**Fig. 11** The effect of length on streamlines

Figure 12 compares the flow conditioner lengths in terms of flow rates for different inlet pressures. Especially at 10 bar inlet pressure, which satisfies the class society rules in terms of both flow rate and throwing distance, the flow conditioner with 100mm length shows the best performance. The difference between the flow rates at constant pressure can also be seen in Figure 12. The streamlines in the fi-fi monitor without any flow conditioner are the worst case that causes the minimum flow rate. With the increase in the flow conditioner length, the streamlines are homogenized until 100mm.

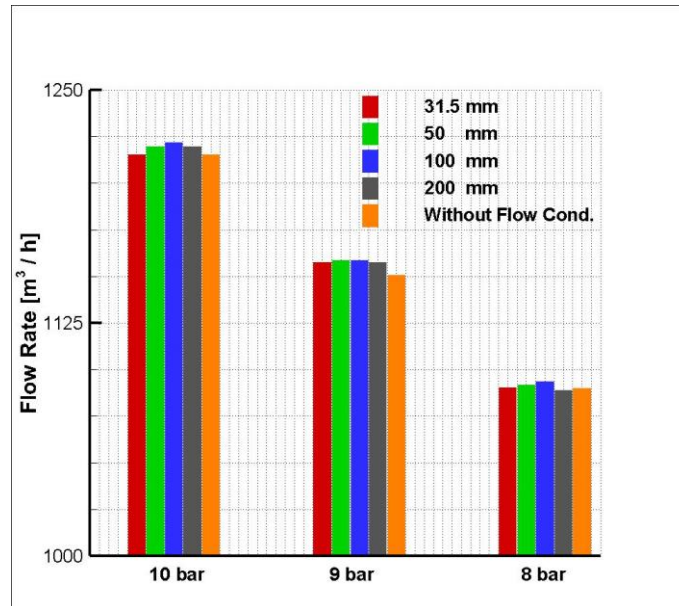


Fig. 12 The effect of length on flow rates

Figure 13 compares the different lengths scenarios considering the head ratio for the unique design. According to this figure, the scenario 100 mm length has the minimum head ratio for all inlet pressures except for without a plate. However, the minimum head ratio is observed when the flow conditioner does not exist. Because the placed flow conditioner in the fi-fi monitor for laminarization is increasing the friction surface area, it is thought that one of the reasons for pressure loss may be caused by this surface area increase.

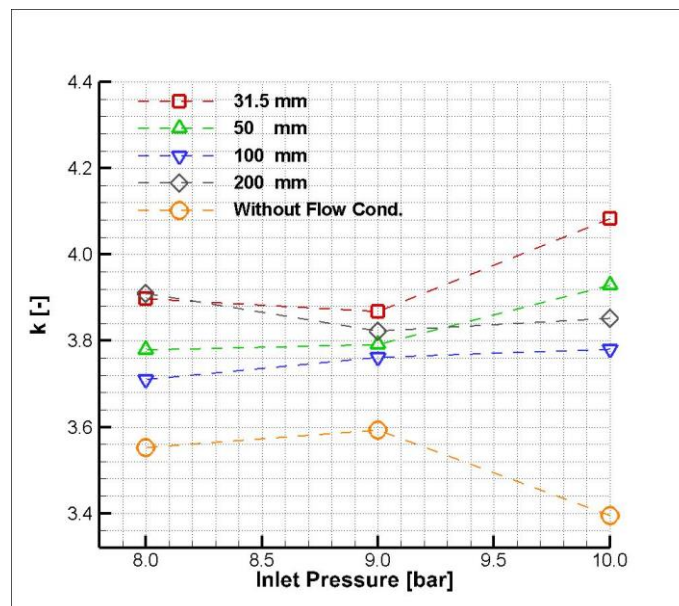


Fig. 13 The effect of length on the head ratio for the unique design

## 6. Conclusion

In the present study, a unique flow conditioner is equipped with the newly designed fi-fi monitor to improve its performance in terms of flow rate and head ratio. To achieve this, firstly the experiments were conducted under the supervision of the Bureau Veritas classification society. Then, a numerical approach based on the finite volume method to discretize unsteady RANS equations was applied and the numerical results were validated with the experiments. The numerical method was also verified spatially and temporally. After the validation, the unique flow conditioner was compared with two different flow conditioners, numerically. Finally, the numerical study was expanded for different lengths for the unique flow conditioner.

The following outcomes are reported in this study:

- After comparing the numerical and experimental results, it is observed that the numerical model can successfully simulate the flow inside the fi-fi monitor. Thus, this numerical model can be a good alternative to the experiments since the experiments are time-consuming and expensive.
- Flow conditioner regulates the flow regardless of the conditioner type by regulating the streamlines.
- The fi-fi monitors without any flow conditioner provide the least flow rate (1215.4 m<sup>3</sup>/h at 10 bar, 1150.5 m<sup>3</sup>/h at 9 bar) comparing the results of different unique flow conditioner lengths.
- The unique flow conditioner equipped with the fi-fi monitor has better results in terms of head ratio ( $k=4.08$ ) although ISO 5167-3 recommends the Zanker ( $k=7.04$ ) and Tube Bundle ( $k=4.39$ ) flow conditioners for 31.5mm flow conditioner length at 10 bar inlet pressure. The same situation is valid at 8-bar and 9-bar inlet pressures.
- Considering the numerical results, the head ratio values for a constant conditioner type and length can be assumed as constant since the effect of inlet pressure on the head ratio is almost negligible.
- When it comes to the flow rate, the unique and tube bundle flow conditioners reach higher flow rate values than the Zanker flow conditioner.
- Although flow conditioner length does not have a remarkable effect on flow rate, the maximum flow rate is observed for 100mm length for tested cases. In addition to this, the same length provides the least head ratio for all inlet pressures. Therefore, a 100mm length seems the most appropriate one for the unique flow conditioner.

The usage of such EFF systems is very crucial and the efficiency of these systems should be of a high standard since there are many serious fire accidents reported in the literature [36]. The proposed design with a unique flow conditioner has acquired BV and TL Marine Type Approval Certificates. Up to now, the product which is the result of this study was used in over 100 commercial and navy vessels. For future work, the effect of fluid type will be investigated for the presented product both experimentally and numerically to see the applicability to other industrial fields. In addition to this, different optimization methods can be employed for parametric optimization as described in [37].

## Acknowledgments

During his Ph.D. study, the first author was funded by the Turkish Council of Higher Education (YÖK). The experiments presented in the study were supported by the Scientific and Technological Research Council of Turkey (TUBITAK) under grant number TEYDEB 7140178 and carried out by Marsis Ltd. under the supervision of Bureau Veritas (BV) and

Turkish Lloyd (TL). The authors want to thank Emre Kahramanoğlu (Ph.D.) for his valuable support.

## REFERENCES

- [1] Rules for the Classification of Steel Ships Part D Service Notations, Chapter 16, Section 3 Machinery and Systems, 2014. Bureau Veritas.
- [2] Benim Haber, 2022, <https://benimhaber.wordpress.com/2012/11/16/meksika-korfezinde-petrol-platformunda-yangin-2-olu/> . accessed 1<sup>st</sup> December 2022.
- [3] T24, 2022. <https://t24.com.tr/haber/haydarpasa-dayanismasi-gar-ne-zaman-acilacak,917656> . accessed 1<sup>st</sup> December 2022
- [4] ISO, 2020. Measurement of fluid flow by means of pressure differential devices inserted in circular cross-section conduits running full-Part 2: Orifice plates (EN ISO 5167-3). European Committee for Standardization, Technical Procedure.
- [5] Brown, G. J., Griffith, B. W., 2013. A New Flow Conditioner for 4-Path Ultrasonic Flowmeters. Paris, France.
- [6] Xiong, W., Kalkühler, K., Merzkirch, W., 2003. Velocity and turbulence measurements downstream of flow conditioners. *Flow Measurement and Instrumentation*, 14(6), 249–260. [https://doi.org/10.1016/S0955-5986\(03\)00031-1](https://doi.org/10.1016/S0955-5986(03)00031-1)
- [7] Laribi, B., Wauters, P., Aichouni, M., 2003. Comparative study of aerodynamic behaviour of three flow conditioners. *European Journal of Mechanical and Environmental Engineering*, 48(1), 21–30.
- [8] Laws, E. M., Ouazzane, A. K., 1995. A further study into the effect of length on the Zanker flow conditioner. *Flow Measurement and Instrumentation*, 6(3), 217–224. [https://doi.org/10.1016/0955-5986\(95\)00010-J](https://doi.org/10.1016/0955-5986(95)00010-J)
- [9] Razali, A. H., Nordin, N., Sapit, A., Alias, Z. A., 2020. Flow through Various Porosity of Circle Grid Perforated Plate with Orifice Plate Flowmeter. *Journal of Complex Flow*, 2(1), 1-6.
- [10] Chen, G., Liu, G., 2018. Performance Evaluation and Analysis of a New Flow Conditioner Based on CFD. *IOP Conference Series: Materials Science and Engineering*, 394, 032049. <https://doi.org/10.1088/1757-899X/394/3/032049>
- [11] Lahadi, M. H., Johari, A. M., Alias, Z. A., 2019. Effect of the Fractal-Grid Generated Turbulence on Turbulent Intensity and Pressure Drop in Pipe Flow. *Journal of Complex Flow*, 1(1), 5-10.
- [12] Pramiyanti, Y., Seri, S. M., Sapit, A., 2020. Incompressible Turbulent Swirling Flow through Circle Grid Perforated Plate. *Journal of Complex Flow*, 2(1), 11-16.
- [13] Zaryankin, A., Rogalev, N., Rogalev, A., Kocherova, A., Kurdiukova, G., 2016. New Flow Stabilizers as a Method to Improve the Reliability and Efficiency of Power Equipment. *Modern Applied Science*, 10(2), 172-184. <https://doi.org/10.5539/mas.v10n2p172>
- [14] Askari, V., Nicolas, D., Edralin, M., Jang, C., 2019. Computational Fluid Dynamics Model for Sensitivity Analysis and Design of Flow Conditioners. *Proceedings of the 9th International Conference on Simulation and Modeling Methodologies, Technologies and Applications*, Prague, Czech Republic. <https://doi.org/10.5220/0007917401290140>
- [15] Bayazit, Y., Sparrow, E. M., Joseph, D. D., 2014. Perforated plates for fluid management: Plate geometry effects and flow regimes. *International Journal of Thermal Science*, 85, 104–111. <https://doi.org/10.1016/j.ijthermalsci.2014.06.002>
- [16] Çarpınlioğlu, M. Ö., Özahi, E., 2011. Laminar flow control via utilization of pipe entrance inserts (a comment on entrance length concept). *Flow Measurement and Instrumentation*, 22(3), 165–174. <https://doi.org/10.1016/j.flowmeasinst.2011.01.005>
- [17] Liu, Q., Tian, S., Lin, Z., Zhu, Z., 2022. Effect of the convergence flow conditioner on rectifying eccentric jet flow induced by a ball valve. *Flow Measurement and Instrumentation*, 83, 102091. <https://doi.org/10.1016/j.flowmeasinst.2021.102091>
- [18] Chen, W., Wu, J., Li, C., 2021. The Investigation on the Flow Distortion Effect of Header to Guarantee the Measurement Accuracy of the Ultrasonic Gas Flowmeter. *Applied Sciences*, 11(8), 3656. <https://doi.org/10.3390/app11083656>



- [19] Hou, Y., Yang, X., Ren, F., Liu, Y., 2018. Structural Analysis and Optimization of Liquid Nitrogen Fire Monitor Based on FLUENT. *3rd International Conference on Electrical, Automation and Mechanical Engineering (EAME 2018)*, Xi'an, China. <https://doi.org/10.2991/eame-18.2018.62>
- [20] Hu, G., Long, M., Liang, J., Li, W., 2012. Analysis of jet characteristics and structural optimization of a liquamatic fire water monitor with self-swinging mechanism. *The International Journal of Advanced Manufacturing Technology*, 59(5–8), 805–813. <https://doi.org/10.1007/s00170-011-3508-y>
- [21] Choudhury, A., Rodriguez, J., 2019. Flow Path Trajectory and Pressure Loss in a Water Monitor Design. *International Journal of Engineering and Manufacturing Science*, 9(2), 89–101.
- [22] Bilir, A. Ç., Doğrul, A., Çoşgun, T., Yurtseven, A., Vardar, N., 2016. A numerical Investigation of the Flow in Water Jet Nozzles. *Journal of Thermal Engineering*, 2(5), 907-912.
- [23] Versteeg, H., Malalasekera, W., 2007. *An Introduction to Computational Fluid Dynamics: The Finite Volume Method*. Harlow, England, New York.
- [24] Menter, F. R., 1993. Zonal Two Equation k-omega Turbulence Models for Aerodynamic Flows. *23rd AIAA Fluid Dynamics, Plasmadynamics and Lasers Conference*, Orlando, Florida, USA. <https://doi.org/10.2514/6.1993-2906>
- [25] Menter, F. R., 1994. Two-Equation Eddy-Viscosity Turbulence Models for Engineering Applications. *AIAA J.*, 32(8), 1598-1605. <https://doi.org/10.2514/3.12149>
- [26] ITTC, 2014. 7.5-03-02-03 Practical Guidelines for Ship CFD Applications. *ITTC - Recommended Procedures and Guidelines*.
- [27] Dogrul, A., 2022. Numerical Prediction of Scale Effects on The Propulsion Performance of JOUBERT BB2 Submarine. *Brodogradnja*, 73(2), 17–42. <https://doi.org/10.21278/brod73202>
- [28] Lijun, D., Meng, H., Qiangzhi, X., Zongjian, H., Baofu, J., Zhiming, W., Jianwen, H., 2021. Numerical analysis of valve structure of high power marine engine. *Brodogradnja*, 72(2), 115-126. <https://doi.org/10.21278/brod72207>
- [29] Cukrov, A., Sato, Y., Boras, I., Ničeno, B. (2021). A solution to Stefan problem using Eulerian two fluid VOF model. *Brodogradnja*, 72(4), 141-164. <https://doi.org/10.21278/brod72408>
- [30] Cosner, R., Oberkampf, B., Rumsey, C., Rahaim, C., Shih, T., 2006. AIAA Committee on Standards for Computational Fluid Dynamics: Status and Plans. *44th AIAA Aerospace Sciences Meeting and Exhibit*, Reno, Nevada, USA. <https://doi.org/10.2514/6.2006-889>
- [31] ITTC, 1999. 7.5-03-01-01 Uncertainty Analysis in CFD, Verification and Validation Methodology and Procedures. *ITTC - Recommended Procedures and Guidelines*.
- [32] Stern, F., Wilson, R. V., Coleman, H. W., Paterson, E. G., 2001. Comprehensive Approach to Verification and Validation of CFD Simulations—Part 1: Methodology and Procedures. *Journal of Fluids Engineering*, 123(4), 793–802. <https://doi.org/10.1115/1.1412235>
- [33] Çelik, I., Ghia, U., Roache, P., Fretias, C. J., Coleman, H., Raad, ve P. E., 2008. Procedure for Estimation and Reporting of Uncertainty Due to Discretization in CFD Applications, *Journal of Fluids Engineering*, 130(7), 078001. <https://doi.org/10.1115/1.2960953>
- [34] P. J. Roache, 1997. Quantification of uncertainty in computational fluid dynamics. *Annual Review of Fluid Mechanics*, vol. 29, 123–160. <https://doi.org/10.1146/annurev.fluid.29.1.123>
- [35] Roache, P. J., 1998. Verification of Codes and Calculations. *AIAA Journal*, 36(5), 696–702. <https://doi.org/10.2514/2.457>
- [36] Barlas, B., Ozsoysal, R., Bayraktarkatal, E., Ozsoysal, O. A., 2017. A study on the identification of fire hazards on board: a case study. *Brodogradnja*, 68(4), 71–87. <https://doi.org/10.21278/brod68405>
- [37] Rodríguez, C. G., Lamas, M. I., Rodríguez, J. D. D., Caccia, C., 2021. Analysis of the pre-injection configuration in a marine engine through several MCDM techniques. *Brodogradnja*, 72(4), 1-17. <https://doi.org/10.21278/brod72401>

Submitted: 06.09.2022. Ahmet Çağrı Bilir  
Yildiz Technical University, Dept. of Naval Arch. and Marine Engineering,  
Istanbul, Türkiye [ahmetcagribilir@gmail.com](mailto:ahmetcagribilir@gmail.com)

Accepted: 02.12.2022. Ali Doğrul, Department of Naval Architecture and Marine Engineering,  
Turkish Naval Academy, National Defense University, 34940, Istanbul,  
Türkiye  
Nurten Vardar, Yildiz Technical University, Dept. of Naval Arch. and Marine  
Engineering, Istanbul, Türkiye